運輸省港湾技術研究所

港湾技術研究所報告

REPORT OF THE PORT AND HARBOUR RESEARCH INSTITUTE

MINISTRY OF TRANSPORT

VOL. 29 NO. 4 DEC. 1990

NAGASE, YOKOSUKA, JAPAN

港湾技術研究所報告 (REPORT OF P.H.R.I.)

第29巻　第4号 (Vol. 29, No. 4) 1990年12月 (Dec. 1990)

目　　次 (CONTENTS)

REPORT OF THE PORT AND
HARBOUR RESEARCH INSTITUTE
Vol. 29, No. 4 (Dec. 1990)

2. Strain Space Plasticity Model for Cyclic Mobility

Susumu IAI*
Yasuo MATSUNAGA**
Tomohiro KAMEOKA**

Synopsis

The cyclic mobility model proposed in this paper is of a generalized plasticity-multiple mechanism type. The salient feature of the present approach is that the concept of the multiple mechanism, within the framework of plasticity theory defined in strain space, is used as a vehicle for decomposing the complex mechanism into a set of one dimensional mechanism. This makes it possible to obtain not only incremental but also integrated constitutive relations. The undrained stress path is idealized with the concept of liquefaction front, which is defined in the effective stress space as an envelope of stress points gradually approaching failure line.

Once coded into the finite element program, most of the existing models suffer from serious difficulty in the numerical solution process when effective stress path becomes very close to the failure line. A numerically robust approach is proposed in this paper by introducing a scheme for gradually enlarging scale of shear strain with the progress of cyclic mobility.

Key words: constitutive equation of soil, dynamic, earthquake, liquefaction, plasticity, sand

* Chier of Geotechnical Earthquake Engineering Laboratory, Structural Engineering Division
** Member of Geotechnical Earthquake Engineering Laboratory, Structural Engineering Division

港湾技術研究所報告
第29巻 第4号 (1990.12)

2. ひずみ空間における塑性論に基づくサイクリックモビリティーのモデル

井合 進*・松永康男**・亀岡知弘**

要 旨

本研究で提案したモデルはマルチメカニズム的な塑性論によるものである。その特徴は，マルチメカニズムの概念を，ひずみ空間で定義された塑性論の枠組みの中でうまく利用して，砂の複雑な力学的機構を複数の一次元的な機構に分解する点にある。これにより，増分型の構成式のみならずこれを積分した形の構成式が得られる。特に，非排水状態での有効応力経路は，液状化フロントという概念を用いてモデル化される。ここに，液状化フロントとは，有効応力空間において定義された一種の包絡線であり，これがサイクリックモビリティーの進行に従って徐々に降伏線に近づくものとしている。

サイクリックモビリティーの数値解析においては，有効応力経路が破壊線に近づくにつれて数値解析上の困難が発生することが知られている。本研究では，サイクリックモビリティーの進行に従って徐々にひずみのスケールを拡大する方法を導入することにより数値解析的な安定性を高めた方法を提案した。

キーワード：液状化／構成式／地震／砂／塑性論／動的

* 構造部地盤震動研究室長
** 構造部地盤震動研究室

CONTENTS

1. Introduction

Two modes have been identified in the earthquake induced damage to soil structures and foundations associated with excess pore water pressure rise in the saturated cohesionless soils. One involves complete flow failure due to loss in the saturated soil strength. This mode of damage is essentially analyzed by the simple static approach within the framework of critical state concept (Castro, 1975); the analysis is done by comparing the post-earthquake residual strength of soil with the initial stress due to gravity. The other involves limited, but often large, amount of deformation due to significant reduction in the soil stiffness but without involving the mechanism of failure in soil. The mechanism for the latter mode of damage is called cyclic mobilty. In practice, cyclic mobility occurring in the looser cohesionless soil is often called 'liquefaction,' which is distinguished from the 'cyclic mobility' occurring in the denser cohesionless soil. In the present paper, both phenomena will be called cyclic mobility as long as the mechanism does not involve the flow failure of soil. For estimating amount of deformation due to cyclic mobility, the dynamic analysis is needed based on a simple but realistic modeling of cyclic mobility.

If a model for cyclic mobility can be of any use in practice of soil dynamics and earthquake engineering, the model may have to be able to simulate rapid or persistent increase in shear strain ranging from about one to ten percent, from which cracks, settlement and other deformation of major consequence initiate. Such a large shear strain is generated only when the effective stress path becomes very close to the failure line. This causes difficulty in the numerical analysis because a very small error contained in the computed effective stress causes a very large error in the computed strains, sometimes causing divergence in the solution process. None of the existing approaches seem to overcome the difficulty. In the present study, an attemptt is made toward achieving the numerical robustness. The model is systematically constructed within the framework of generalized plasticity theory defined in the strain space.

2. Generalized Plasticity Theory in Strain Space

Behavior of saturated cohesionless soil is defined in terms of effective stress and strain. If vector-matrix notation is used, the effective stress increment $d\sigma'$ and the strain increment $d\varepsilon$ are related with each other through the tangential stiffness matrix D as

$$d\sigma' = D d\varepsilon \tag{1}$$

At each stage of deformation process under transient and cyclic loads, a direction is introduced which differentiates loading from unloading (i. e. reversal loading). Commonly adopted practice is to define the direction in the stress space but, in the present study, the direction n is introduced in the strain space as suggested by Mroz and Norris (1982). The dependence of the material behvior on the direction is specified by writing

$$\begin{aligned} d\sigma' &= D_L d\varepsilon \quad \text{if } n^T d\varepsilon > 0 \\ d\sigma' &= D_U d\varepsilon \quad \text{if } n^T d\varepsilon < 0 \end{aligned} \tag{2}$$

Models of this type can be generalized further by considering that the deformation of material is produced by $I+1$ separate mechanisms with $i=0, 1, \cdots\cdots, I$, all of which are subjected to the same state and history of strain. In this approach increment of effective stress is written as

$$d\boldsymbol{\sigma}' = \sum_{i=0}^{I} d\boldsymbol{\sigma}'^{(i)} \tag{3}$$

and is related to the increment of strain by

$$d\boldsymbol{\sigma}' = \sum_{i=0}^{I} \boldsymbol{D}^{(i)} d\boldsymbol{\varepsilon} \tag{4}$$

Dependence of the material behavior on the direction of loading is separately defined for each mechanism, such that

$$\begin{aligned} d\boldsymbol{\sigma}'^{(i)} &= \boldsymbol{D}_L{}^{(i)} d\boldsymbol{\varepsilon} \qquad \text{if } \boldsymbol{n}^{(i)T} d\boldsymbol{\varepsilon} > 0 \\ d\boldsymbol{\sigma}'^{(i)} &= \boldsymbol{D}_U{}^{(i)} d\boldsymbol{\varepsilon} \qquad \text{if } \boldsymbol{n}^{(i)T} d\boldsymbol{\varepsilon} < 0 \end{aligned} \tag{5}$$

The plasticity theory in strain space, which assures the uniqueness of stress increment $d\boldsymbol{\sigma}'^{(i)}$ for each mechanism, demands that $\boldsymbol{D}_{L/U}{}^{(i)}$ is specified by

$$\begin{aligned} \boldsymbol{D}_L{}^{(i)} &= R_L{}^{(i)} \boldsymbol{n}_L{}^{(i)} \boldsymbol{n}^{(i)T} \\ \boldsymbol{D}_U{}^{(i)} &= R_U{}^{(i)} \boldsymbol{n}_U{}^{(i)} \boldsymbol{n}^{(i)T} \end{aligned} \tag{6}$$

in which $\boldsymbol{n}_{L/U}{}^{(i)}$ are arbitrarily specified vector definig the directions of stress increments and the scalars $R_{L/U}{}^{(i)}$ define the magnitudes of stress increments. Thus, the constitutive relation is given by

$$d\boldsymbol{\sigma}' = \sum_{i=0}^{I} R_{L/U}{}^{(i)} \boldsymbol{n}_{L/U}{}^{(i)} \boldsymbol{n}^{(i)T} d\boldsymbol{\varepsilon} \tag{7}$$

in which L/U is determined for each mechanism by Eq. (5).

3. Decomposition into Simple Mechanisms

In attempting to construct the model for cyclic mobility with practical application in mind, the author limits himself, throughout the following discussion, to the two dimensional behavior of soil under plane strain condition. Thus, the components of the effective stress and the strain vectors are given as

$$\boldsymbol{\sigma}'^{T} = (\sigma_x', \sigma_y', \tau_{xy}) \tag{8}$$

$$\boldsymbol{\varepsilon}^{T} = (\varepsilon_x, \varepsilon_y, \gamma_{xy}) \tag{9}$$

in which compressive stress and contractive strain will be assumed negative and the strains will be given from displacements u and v in x and y directions as

$$\varepsilon_x = \frac{\partial u}{\partial x}, \quad \varepsilon_y = \frac{\partial v}{\partial y}, \quad \gamma_{xy} = \frac{\partial u}{\partial y} + \frac{\partial v}{\partial x} \tag{10}$$

It is assumed in the following discussion that σ_z' is approximately equal to $(\sigma_x' + \sigma_y')/2$.

3.1 Transformation

The first step to take for developing the model is to decompose the mechanism of cyclic mobility into two mechanisms; one being the mechanism of cumulative pore pressure build up with occasional recovery of mean effective stress, the other the mechanism of shear deformation without volume change.

Such decomposition is most conveniently done if we at first transform the effective stress and the strain vectors into vectors with components of volumetric nature and shear nature as follows. The effective stress vector is transformed as

$$\boldsymbol{s}' = \boldsymbol{T}_\sigma \boldsymbol{\sigma}' \tag{11}$$

in which

$$\boldsymbol{s}'^T = [(\sigma_x' + \sigma_y')/2,\ (\sigma_x' - \sigma_y')/2,\ \tau_{xy}] \tag{12}$$

$$\boldsymbol{T}_\sigma = \begin{bmatrix} \frac{1}{2} & \frac{1}{2} & 0 \\ \frac{1}{2} & -\frac{1}{2} & 0 \\ 0 & 0 & 1 \end{bmatrix} \tag{13}$$

and the strain vector is transformed as

$$\boldsymbol{e} = \boldsymbol{T}_\varepsilon \boldsymbol{\varepsilon} \tag{14}$$

in which

$$\boldsymbol{e}^T = [(\varepsilon_x + \varepsilon_y),\ (\varepsilon_x - \varepsilon_y),\ \gamma_{xy}] \tag{15}$$

$$\boldsymbol{T}_\varepsilon = \begin{bmatrix} 1 & 1 & 0 \\ 1 & -1 & 0 \\ 0 & 0 & 1 \end{bmatrix} \tag{16}$$

It is to be noted that $\boldsymbol{T}_\sigma$ and $\boldsymbol{T}_\varepsilon$ are related with each other by

$$\boldsymbol{T}_\sigma^T = \boldsymbol{T}_\varepsilon^{-1} \tag{17}$$

By using Eqs. (11), (14) and (17), the constitutive relation in Eq. (7) is rewritten as

$$d\boldsymbol{s}' = \sum_{i=0}^{I} R_{L/U}{}^{(i)}\, \boldsymbol{T}_\sigma \boldsymbol{n}_{L/U}{}^{(i)} \boldsymbol{n}^{(i)T} \boldsymbol{T}_\sigma^T d\boldsymbol{e} \tag{18}$$

If we define the direction vectors in the transformed space as

$$\begin{aligned} \boldsymbol{l}_{L/U}{}^{(i)} &= \boldsymbol{T}_\sigma \boldsymbol{n}_{L/U}{}^{(i)} \\ \boldsymbol{l}^{(i)} &= \boldsymbol{T}_\sigma \boldsymbol{n}^{(i)} \end{aligned} \tag{19}$$

Eq. (18) is rewritten as

$$d\boldsymbol{s}' = \sum_{i=0}^{I} R_{L/U}{}^{(i)} \boldsymbol{l}_{L/U}{}^{(i)} \boldsymbol{l}^{(i)T} d\boldsymbol{e} \tag{20}$$

Eqs. (7) and (20) are the dual representation of the constitutive relation and, if we prescribe $R_{L/U}{}^{(i)}$, $\boldsymbol{l}_{L/U}{}^{(i)}$ and $\boldsymbol{l}^{(i)}$ in the transformed space, $\boldsymbol{n}_{L/U}{}^{(i)}$ and $\boldsymbol{n}^{(i)}$ will readily be given in the original space by Eqs. (17) and (19) and consequently Eq. (7) is completely specified.

3.2 Volumetric Mechanism

With the Eq. (20) in hand, the first mechanism (i.e. the mechanism for $j=0$) will be defined for representing the cumulative pore pressure build up with occasional recovery of mean effective stress. For modeling such a mechanism, the author takes the approach similar, in principle, to that taken for densification model (Zienkiewicz et al, 1978). This approach has the advantage of simplicity and of the most direct use of the laboratory data obtained under cyclic loading condition. In this approach, we need simply to include an additional strain $\boldsymbol{e}_p$ of volumetric nature into the mechanism for $i=0$ in Eq. (20) by writing

$$d\boldsymbol{s}'^{(0)} = R_{L/U}{}^{(0)} \boldsymbol{l}_{L/U}{}^{(0)} \boldsymbol{l}^{(0)T} (d\boldsymbol{e} - d\boldsymbol{e}_p) \tag{21}$$

in which $d\boldsymbol{e}_p$ will be independently determined.

Since the mean effective stress and the volumetric strain are the first components of $\boldsymbol{s}'$ and $\boldsymbol{e}$, the direction vectors in Eq. (21) are given as

$$\boldsymbol{l}^{(0)T} = \boldsymbol{l}_U{}^{(0)T} = \boldsymbol{l}^{(0)T} = (1,\ 0,\ 0) \tag{22}$$

with the additional volumetric strain given as

$$\boldsymbol{e}_p{}^T = (\varepsilon_p,\ 0,\ 0) \tag{23}$$

The additional volumetric strain $\boldsymbol{e}_p$ is further assumed to reprsent whole part of plastic volumetric strain generated by transient and cyclic loads. Then the strain increment $\boldsymbol{l}^{(0)T}(d\boldsymbol{e} - d\boldsymbol{e}_p)$ in Eq. (21) becomes elastic so that the moduli $R_{L/U}{}^{(0)}$ in Eq. (21) should represent elastic volumetric behavior, i.e.

$$K = R_L{}^{(0)} = R_U{}^{(0)} \tag{24}$$

in which K is elastic tangent bulk modulus of soil skeleton, often called rebound modulus. The laboratory data suggest that, for cohesionless soil, K is given by a power function of effective mean stress, approximately given as

$$K = K_a (\sigma_m'/\sigma_{ma}')^{0.5} \tag{25}$$

in whch σ_m': effective mean stress $=(\sigma_x'+\sigma_y')/2$; K_a: elastic tangent bulk modulus of soil skeleton at $\sigma_m' = \sigma_{ma}'$; and σ_{ma}': effective mean stress at which K is defined as $K = K_a$.

3.3 Shear Mechanism

The frame work for the first mechanism thus defined, the second mechanism will be defined for representing the shear deformation without volume change. For modeling such a mechanism, the author adopts the approach similar to that proposed by Towhata and Ishihara (1985 a). This approach has the advantage of representing soil behavior under principal stress axes rotation. This approach, at the same time, has the advantage of simplicity by decomposing the complex mechanism into a set of such simple mechanisms as those defined in one dimensional space.

In this approach, we need to mobilize I mechanisms for $i=1,\cdots\cdots,I$ out of Eq. (20) by writing

$$\sum_{i=1}^{I} d\boldsymbol{s}'^{(i)} = \sum_{i=1}^{I} R_{L/U}{}^{(i)} \boldsymbol{l}_{L/U}{}^{(i)} \boldsymbol{l}^{(i)T} d\boldsymbol{e} \tag{26}$$

as a tool for the decomposition. The mechanism i represents a one dimensional stress strain relation defined in a virtual simple shear which is, in concept, mobilized at angle $\theta_i/2+\pi/4$ to the x axis; e.g. the mechanism with $\theta_i=0$ represents a virtual compression mode, that with $\theta_i=\pi/2$ representing a virtual simple shear mode in the x axis direction

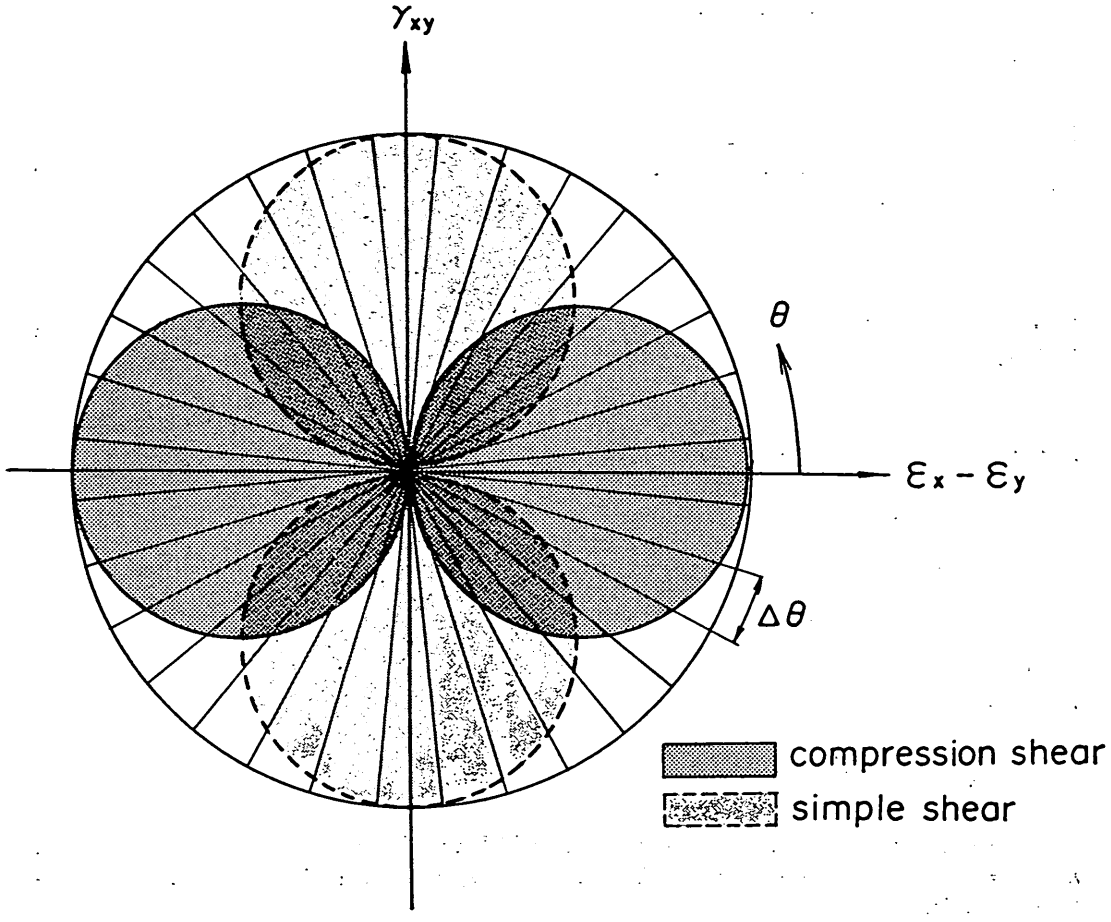

Fig. 1 Schematic figure for multiple simple shear mechanisms (pairs of circles indicate mobilized virtual shear strain in positive and negative modes of compression shear and simple shear)

as shown in **Fig. 1.** The angle θ_i for mechanism i is given so that all the possible directions for mobilization are approximately represented by those of I mechanisms, such that

$$\theta_i=(i-1)\Delta\theta \qquad (\text{for } i=1,\cdots\cdots, I) \tag{27}$$

in which $\Delta\theta=\pi/I$.

The above definition of mechanism i demands, as shown in **Fig. 1,** that the direction vectors in Eq. (26) be given by

$$\boldsymbol{l}_L^{(i)T}=\boldsymbol{l}_U^{(i)T}=\boldsymbol{l}^{(i)T}=(0,\ \cos\theta_i,\ \sin\theta_i) \qquad (\text{for } i=1,\cdots\cdots, I) \tag{28}$$

with $R_{L/U}^{(i)}$ representing tangent shear moduli which will be given as a function of virtual simple shear strain for mechanism i (i.e. $\boldsymbol{l}^{(i)T}\boldsymbol{e}$) and of its history.

3.4 Incremental Relation

If the expressions for the mechanisms given by Eqs. (21) and (26) are combined, a

relation which corresponds to Eq. (20) is given as

$$d\boldsymbol{s}' = K\boldsymbol{l}^{(0)}\boldsymbol{l}^{(0)T}(d\boldsymbol{e} - d\boldsymbol{e}_p) + \sum_{i=1}^{I} R_{L/R}{}^{(i)}\boldsymbol{l}^{(i)}\boldsymbol{l}^{(i)T}d\boldsymbol{e} \tag{29}$$

in which modulus K is defined by Eq. (25), the direction vectors by Eqs. (22) and (28).

As mentioned earlier, the constitutive relation in Eq. (26) is back-transformed into the original representation corresponding to Eq. (7) as

$$d\boldsymbol{\sigma}' = K\boldsymbol{n}^{(0)}\boldsymbol{n}^{(0)T}(d\boldsymbol{\varepsilon} - d\boldsymbol{\varepsilon}_p) + \sum_{i=1}^{I} R_{L/U}{}^{(i)}\boldsymbol{n}^{(i)}\boldsymbol{n}^{(i)T}d\boldsymbol{\varepsilon} \tag{30}$$

in which volumetric strain increment $d\boldsymbol{\varepsilon}_p$ of plastic nature is given, by using the relation in Eqs. (14) and (17), as

$$d\boldsymbol{\varepsilon}_p = \boldsymbol{T}_o{}^T d\boldsymbol{e}_p \tag{31}$$

and the direction vectors in the original space $\boldsymbol{n}^{(i)}$ are given by Eqs. (17) and (19) as

$$\boldsymbol{n}^{(0)T} = (1,\ 1,\ 0) \tag{32}$$

$$\boldsymbol{n}^{(i)T} = (\cos\theta_i,\ -\cos\theta_i,\ \sin\theta_i) \qquad (\text{for } i=1, \cdots\cdots, I) \tag{33}$$

Because $\boldsymbol{n}^{(i)}d\boldsymbol{\varepsilon}_p = 0$ for $i=1, \cdots\cdots, I$, Eq. (30) is rewritten as

$$d\boldsymbol{\sigma} = \boldsymbol{D}(d\boldsymbol{\varepsilon} - d\boldsymbol{\varepsilon}_p) \tag{34}$$

in which

$$\boldsymbol{D} = K\boldsymbol{n}^{(i)}\boldsymbol{n}^{(0)T} + \sum_{i=1}^{I} R_{L/U}{}^{(i)}\boldsymbol{n}^{(i)}\boldsymbol{n}^{(i)T} \tag{35}$$

As expected from the associative manner with which the direction vectors are chosen (i.e. $\boldsymbol{n}_{L/U}{}^{(i)} = \boldsymbol{n}^{(i)}$), the stiffness matrix $\boldsymbol{D}$ in Eq. (34) is symmetric, giving the advantage of efficient solution.

4. Integrated Formulation

The decomposition into one dimensional mechanisms in Eq. (30) provides a salient feature in the present approach; the incremental relation can be integrated so that a direct relation can be specified between effective stress and strain. Such integration can be done one by one with respect to each variable defined for each mechanism.

The mechanism $i=0$ in Eq. (29) can be rewritten as

$$d\sigma_m' = K_a(\sigma_m'/\sigma_{ma}')^{0.5}d\varepsilon_e \tag{36}$$

in which elastic volumetric strain increment $d\varepsilon_e$ is defined as

$$d\varepsilon_e = \boldsymbol{l}^{(0)T}(d\boldsymbol{e} - d\boldsymbol{e}_p) \tag{37}$$

Integration of Eq. (36) into the compressive side (i.e. into the negative side) with the conditions that $\varepsilon_e = 0$ when $\sigma_m' = 0$ yields

$$\sigma_m' = -B(-\varepsilon_e)^2 \tag{38}$$

in which

$$B=[0.5K_a/(-\sigma_{ma}')^{0.5}]^2 \tag{39}$$

$$\varepsilon_e=\varepsilon_x+\varepsilon_y-\varepsilon_p \tag{40}$$

The integrated result can be written back in the multiple mechanism formulation similar to Eq. (21) as

$$\boldsymbol{s}'^{(0)}=-B(-\varepsilon_e)^2\boldsymbol{n}^{(0)} \tag{41}$$

The transformation back to the original space by using Eqs. (11) and (19) yields

$$\boldsymbol{\sigma}'^{(0)}=-B(-\varepsilon_e)^2\boldsymbol{n}^{(0)} \tag{42}$$

This is the integrated relation for the mechanism $i=0$.

The rest of the mechanisms $i=1, \cdots\cdots, I$ are integrated by introducing virtual shear strain for each mechanism i as

$$\begin{aligned}\gamma^{(i)}&=\boldsymbol{l}^{(i)T}\boldsymbol{e}\\&=(\varepsilon_x-\varepsilon_y)\cos\theta_i+\gamma_{xy}\sin\theta_i\end{aligned} \tag{43}$$

and by introducing a scalar function $Q^{(i)}(\gamma^{(i)})$ defined so that its first order derivative $\dfrac{dQ^{(i)}}{d\gamma^{(i)}}$ represents the virtual tangent shear moduli per unit angle of θ as

$$R_{L/U}{}^{(i)}=\frac{dQ^{(i)}}{d\gamma^{(i)}}\Delta\theta \tag{44}$$

in which $\Delta\theta=\pi/I$. The value of $Q^{(i)}$ in general depends on the history of $\gamma^{(i)}$. Analogously to the integration of mechanism $i=0$, the mechanisms $i=1, \cdots\cdots, I$ in Eq. (26) is rewritten by using Eqs. (43) and (44) as

$$d\boldsymbol{s}'^{(i)}=\frac{dQ^{(i)}}{d\gamma^{(i)}}\Delta\theta d\gamma^{(i)}\boldsymbol{l}^{(i)} \tag{45}$$

Integration of Eq. (45) yields

$$\boldsymbol{s}'^{(i)}=Q^{(i)}(\gamma^{(i)})\Delta\theta\boldsymbol{l}^{(i)} \tag{46}$$

The transformation back to the original space by using Eqs. (11) and (19) yields

$$\boldsymbol{\sigma}'^{(i)}=Q^{(i)}(\gamma^{(i)})\Delta\theta\boldsymbol{n}^{(i)} \tag{47}$$

From Eqs. (40), (42) and (47), one obtains the integrated formulation for the stress and strain relation as

$$\boldsymbol{\sigma}'=-B[\varepsilon_p-(\varepsilon_x+\varepsilon_y)]^2\boldsymbol{n}^{(0)}+\sum_{i=1}^{I}Q^{(i)}(\gamma^{(i)})\Delta\theta\boldsymbol{n}^{(i)} \tag{48}$$

in which, as mentioned earlier, the value of the function $Q^{(i)}(\gamma^{(i)})$ generally depends on the value as well as history of the variable $\gamma^{(i)}$. The function $Q^{(i)}$ can be interpreted as virtual shear stress per unit angle θ for mechanism i.

Now that incremental as well as integrated relation for modeling cyclic mobility is obtained in the previous and the present sections, it remains to define the volumetric strain ε_p of plastic nature and the function $Q^{(i)}(\gamma^{(i)})$ for representing the virtual shear mechanism.

5. Undrained Effective Stress Path

5.1 Effective Mean Stress Change

General understanding on the liquefaction and cyclic mobility of saturated cohesionless soil is that cyclic loading induces a soil particle rearrangement causing, under drained condition, volumetric shrinkage. Such a rearrangement causes, under undrained condition, loss in effective mean stress and increase in pore water pressure.

In order to formulate this relation, let us consider the mechanism of undrained behavior of cohesionless soil. For simplicity, let us assume that the volumetric strain ε_p of plastic nature is zero at the initial condition. The initial elastic volumetric strain ε_{e0} is related

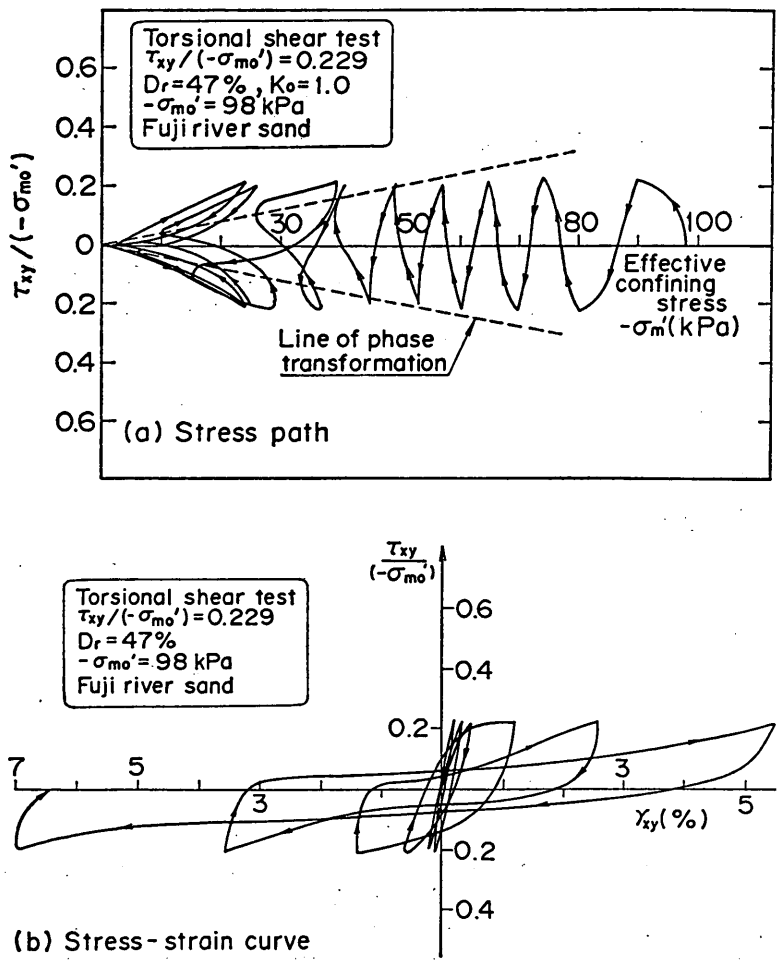

Fig. 2 Stress path and stress-strain curve for loose sand obtaind from the cyclic torsion shear test (aftter Ishihara, 1985)

to the initial effective mean stress σ_{m0}' via Eq. (38) as

$$\sigma_{m0}' = -B(-\varepsilon_{e0})^2 \tag{49}$$

Under constant total mean stress with undrained condition, volumetric strain induced by the change in the effective stress is only due to the volumetric strain of pore water, such that

$$\varepsilon_e + \varepsilon_p - \varepsilon_{e0} = (n/K_f)(\sigma_{m0}' - \sigma_m') \tag{50}$$

in which n and K_f are the porosity of soil skeleton and the bulk modulus of pore water. Elimination of ε_e from Eq. (50) by using Eq. (38) yields

$$\varepsilon_p = (n/K_f)(\sigma_{m0}' - \sigma_m') + [\sigma_m'/(-B)]^{0.5} + \varepsilon_{e0} \tag{51}$$

Whereas volumetric strain ε_p of plastic nature is needed to be specified in Eq. (48), common practice in soil dynamics and earthquake engineering is to measure pore water pressure change or, equivalently, to measure change in effective mean stress under undrained cyclic

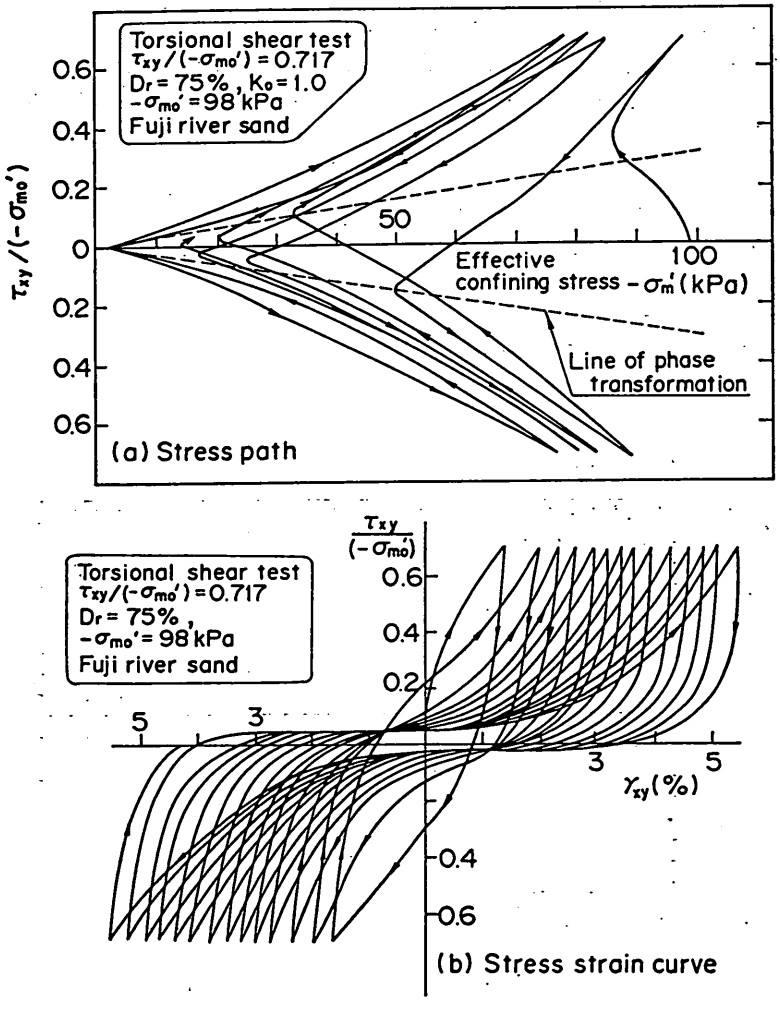

Fig. 3 Stress path and stress-strain curve for dense sand obtained from the cyclic torsion shear test (after Ishihara, 1985)

loading condition. Since one quantity is related with the others by Eq. (51), the measurable quantity, i.e. the undrained effective mean stress change under constant total confining pressure, will be used in the following formulation.

5.2 Liquefaction Front

Several attempts have been made for modeling effective stress paths for cyclic mobility, such as shown in **Figs. 2** and **3**, under undrained cyclic loading condition. Pender (1980), paying due attention to the critical state, adopted parabolic function. Ishihara and Towhata (1982), paying due attention to the yield loci and phase transformation line, adopted combination of parabolic and hyperbolic functions. Yamazaki et al (1985), paying due attention to the envelope of stress points specified by equally accumulated shear work, adopted hyperbolic functions.

In the present study, the author postulates that the phase transformation line and the envelope of stress points at equal shear work are two of the key concepts for modeling effective stress path associated with the cyclic mobility. The phase transformation line as defined by Ishihara et al (1975) is a straight line differentiating a dilative zone in the stress space from contractive zone as indicated by broken lines in **Figs. 2** and **3.** The envelope of sterss points at equal shear work as defined by Towhata and Isihara (1985 b) is represented by a contour, as shown in **Fig. 4**, defined in the stress space at which cumulative shear work is equal to a specified value. As shear work is accumulated by cyclic shear under undrained condition, the envelope of stress points at equal shear work gradually moves from the initial envelope to the failure line. Such an envelope, being one of the key concepts for modeling cyclic mobility, will be called "liquefaction front" in the following discussion.

In order to generalize the formulation of liquefaction front, the liquefaction front will defined in the normalized stress space defined with the effective mean stress ratio $S=\sigma_m'/\sigma_{m0}'$ and the deviatoric stress ratio $r=\tau/(-\sigma_{m0}')$; in which $\sigma_{m0}'=(\sigma_{x0}'+\sigma_{y0}')/2$ is the initial effective mean stress and the deviatoric stress is defined by $\tau=(\sigma_1'-\sigma_3')/2=\sqrt{\tau_{xy}^2+[(\sigma_x'-\sigma_y')/2]^2}$. In principle the shape of the liquefaction front may be approximated by two segments of straight lines in the stress space as indicated by

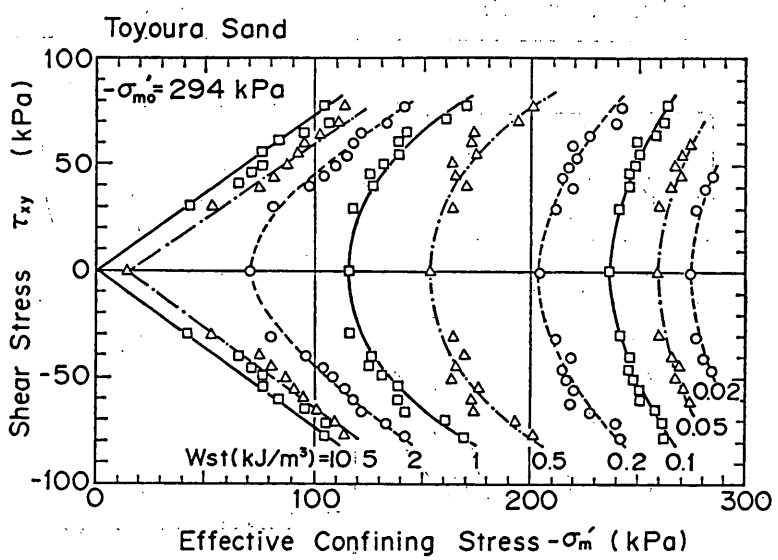

Fig. 4 Envelope of stress points at equal shear work (after Towhata and Ishihara, 1985b)

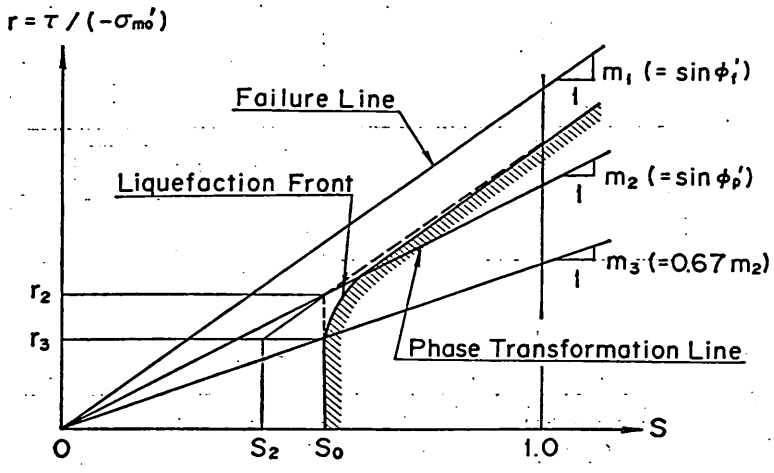

Fig. 5 Schematic figure of liquefaction front, state variable S and shear stress ratio r

the broken line segments in **Fig. 5**; one being the segment of a vertical line defined in the contractive zone, the other being the segment of a line parallel to the failure line defined in the dilative zone. In practice, however, a smooth transition from one zone to the other is necessary for assuring easy and reliable numerical solution. Thus the shape of the liquefaction front will be approximated, as shown in **Fig. 5**, by the following function:

$$S=S_0 \qquad (\text{if } r<r_3)$$
$$S=S_2+\sqrt{(S_0-S_2)^2+[(r-r_3)/m_1]^2} \qquad (\text{if } r>r_3) \tag{52}$$

in which

$$r_2=m_2S_0 \tag{53}$$

$$r_3=m_3S_0 \tag{54}$$

$$S_2=S_0-(r_2-r_3)m_1 \tag{55}$$

and S_0 : a parameter to be defined by a function of shear work; m_1 : inclination of failure line, defined by the shear resistance angle ϕ_f' as $m_1=\sin\phi_f'$; m_2 : inclination of phase transformation line, defined by the phase transformation angle ϕ_p' as $m_2=\sin\phi_p'$; and $m_3=0.67\,m_2$. The auxiliary parameter m_3, introduced for assuring the smooth transition from one zone to the other, is determined as a balance of the smoothness and the realistic stress path shape.

In this formulation, the parameter S_0, hereafter called "liquefaction front parameter," may well be interpreted as a measure which defines the state of liquefaction; e. g. $S_0=1.0$ being the initial stress state if $r<m_3$, $S_0=0$ being the limiting state at which failure occurs due to liquefaction. At a certain boundary value problem, initial shear ratio can be very high so that $r>m_3$. In such a case, initial value of the liquefaction front parameter S_0 should be determined from the initial value of r by solving the second equation in Eq. (52) with $S=1.0$. S_0 is easily obtained as a solution of second order polynomial equation.

5.3 Shear Work Correlation

The liqnefaction front parameter S_0 is given by a function of shear work. Towhata and

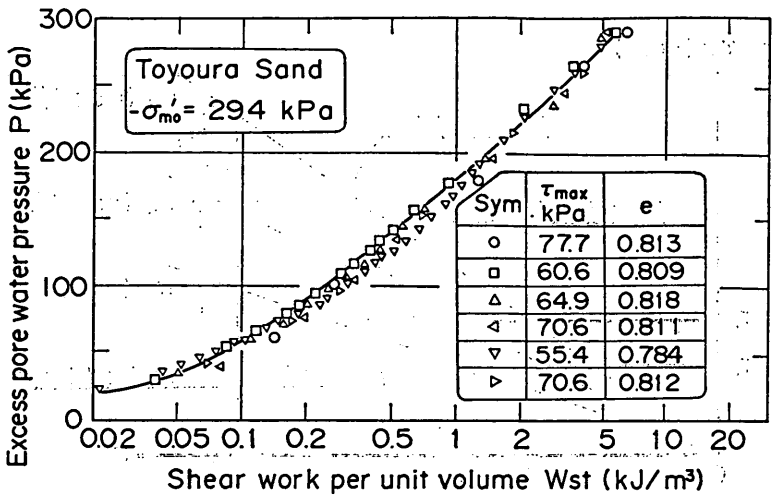

Fig. 6 Correlation between the shear work and the excess pore water pressure (after Towhata and Ishihara, 1985b)

Ishihara (1985 b) obtained the correlation between the shear work and the excess pore water pressure such as shown in **Fig. 6** and concluded that the correlation is independent of the shear stress paths with or without the rotation of principal stress axes. This correlation is generalized by defining a relation between the liquefaction front parameter S_0 and the normalized shear work defined by

$$w = W_s / W_n \tag{56}$$

The factor for normalization W_n is given by

$$W_n = \tau_{m0}\gamma_{m0}/2 \tag{57}$$

in which τ_{m0} and γ_{m0} are drained shear strength and reference strain, at the initial effective mean stress σ_{m0}, to be defined with the initial shear modulus G_{m0} as

$$\tau_{m0} = (-\sigma_{m0}') \sin \phi_f' \tag{58}$$

$$\gamma_{m0} = \tau_{m0}/G_{m0} \tag{59}$$

The initial shear mcdulus of cohesionless soil is known to be given by a power function of effective mean stress, approximated as

$$G_{m0} = G_{ma}(\sigma_{m0}'/\sigma_{ma}')^{0.5} \tag{60}$$

in which G_{ma}: initial shear modulus at $\sigma_{m0}' = \sigma_{ma}'$; and σ_{ma}': effective mean stress at which G_{ma} is defined $G_{m0} = G_{ma}$.

With such a normalization for shear work, the correlation between the liquefaction parameter and the normalized shear work can be empirically modeled based on the following considerations:

(1) Certain laboratory studies indicate a "break" at $S_0 = 0.4$ (Zienkiewicz et al, 1978) from which the behavior of soil drastically change. Therefore, it would be desirable to express the correlation with two functions; one defined for $S_0 > 0.4$, the other for $S_0 < 0.4$. Thus, at least two parameters are necessary.

(2) In order to fit the model to a set of soils with various degree of liquefaction resistance,

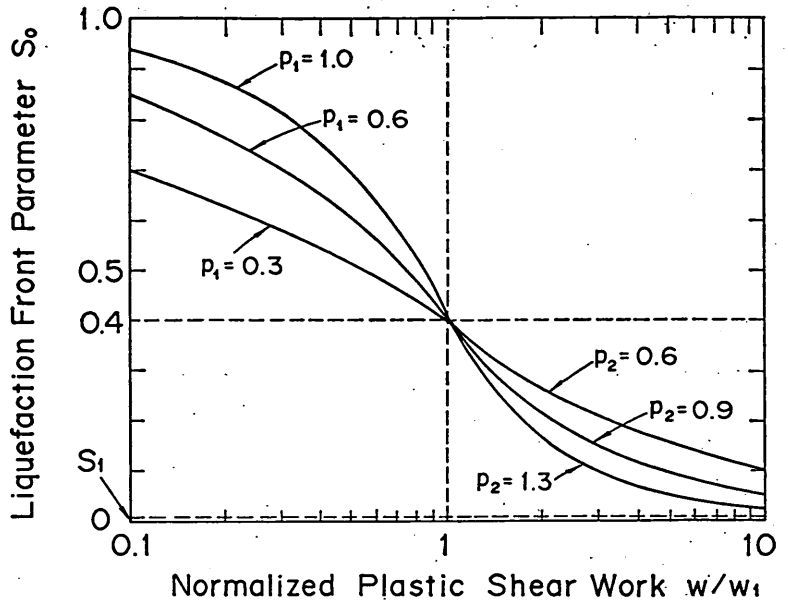

Fig. 7 Relation between normalized plastic shear work w and liquefaction front parameter S_0

it would be desirable to have a parameter which can control, over the entire zone of S_0, the contribution of normalized shear work. This adds one parameter.
(3) In the limiting case S_0 should not become zero if stable simulatlon of cyclic mobility is needed. This indicates use of small parameter is needed as the limiting value for S_0. This adds another parameter.

Based on the above considerations, the correlation between the liquefaction front parameter and the normalized shear work is given with four parameters, such that

$$S_0=1-0.6(w/w_1)p_1 \qquad (\text{if } w<w_1)$$
$$S_0=(0.4-S_1)(w_1/w)p_2+S_1 \qquad (\text{if } w>w_1) \tag{61}$$

in which S_1, w_1, p_1 and p_2 are the material parameters which characterize the liquefaction properties of the cohesionless soil. The schematic figure is shown in **Fig. 7**.

5.4 Threshold Limit

In obtaining the shear work correlation, Towhata and Ishihara (1985 b) used total shear work such as

$$dW_{st}=[(\sigma_x'-\sigma_y')/2]d(\varepsilon_x-\varepsilon_y)+\tau_{xy}d\gamma_{xy} \tag{62}$$

It is assumed in Eq.(62) that dW_{st} is always positive so that, if the right hand side should take negative value, its absolute is taken. The use of total shear work gave satisfactory correlation for the range of test data studied by Towhata and Ishihara (1985 b). It is known, however, that there exists a threshold limit in the amplitude of cyclic shear strain or shear stress; for cyclic strain or stress below this threshold level, there is no pore water pressure build-up (Dobry, et al, 1982). In order to incorporate such a factor of practical significance into the correlation by Eq. (61), the shear work which would be consumed by the threshold limit will be subtracted from the total shear work. Because the shear work

consumed by the threshold limit may be closely related with the elastic shear work, it will be given by introducing a parameter c_1 for specifying the threshold level as

$$c_1 dW_{se} = c_1 |\tau d(\tau / G_m^*)| \tag{63}$$

in which G_m^*: elastic modulus at effective mean stress σ_m' given as

$$G_m^* = G_{m0}(\sigma_m'/\sigma_{m0}')^{0.5} \tag{64}$$

Thus the shear work increment to be used for the shear work correlation in Eq. (61) is given by

$$dW_s = dW_{st} - c_1 dW_{se} \tag{65}$$

It is understood in Eq. (65) that, if the value of right hand side should become negative, dW_s will be assumed zero. In general shear work induced by plastic strain is called plastic shear work. The shear work W_s defined in Eq. (65) is in its approximate sense total shear work minus elastic shear work. Therefore, in the following discussion, the shear work W_s will be conveniently called "plastic shear work".

In the formulation presented so far, the plastic shear work always contributes to the progress of liquefaction whether the effective stress is in the dilative zone or the contractive zone. It is believed, however, that not all the plastic shear work induced in the dilative zone contributes to the progress of liquefaction. In a pragmatic sense this fact is already incorporated in the shear work correlation in Eq. (61). The author believes, however, that some explicit correction for shear work increment is needed in the dilative zone. Such a correction is described in the Appendix.

At each stage of deformation process under transient and cyclic loads, increment in plastic shear work will be computed via Eq. (65) (with the correction in the Appendix when in dilative zone). The accumulated plastic shear work W_s will be normalized by Eq. (56) and substituted into Eq. (61), giving the liquefaction front parameter S_0. From the liquefaction front parameter S_0 and the deviatoric stress ratio r, the effective mean stress ratio S will be obtained by Eq. (52). Finally the effective mean stress ratio S is multiplied by initial mean effective stress σ_{m0}', giving the volumetric strain ε_p of plastic nature by Eq. (51).

In closing this section, it should be cautioned that such variables as σ_m' and S are used in this section in the context of undrained tests under constant total stress. Such tests are considered only as a mean to establish the relation between the shear work and the volumetric strain ε_p of plastic nature. Therefore, when those variables are computed from plastic shear work, they should be regarded as state variables rather than real variables to be computed as a solution of boundary value problems.

6. Shear Mechanism

In defining the virtual tangent shear moduli $R_{L/U}^{(i)}$ in Eq. (30) and the virtual shear stress $Q^{(i)}(\gamma^{(i)})$ in Eq. (48), it is assumed that each virtual simple shear mechanism can be approximated by the one dimensional stress strain relation observed in the actual simple shear test. As a candidate for such one dimensional relation, the hyperbolic stress strain relation is adopted for initial or monotonic loading as

$$Q^{(i)}(\gamma^{(i)}) = [(\gamma^{(i)}/\gamma_v^{(i)})/(1+|\gamma^{(i)}/\gamma_v^{(i)}|)]Q_v^{(i)} \tag{66}$$

in which $Q_v^{(i)}$: virtual shear strength for mechanism i; and $\gamma_v^{(i)}$: virtual reference strain. For simplicity, material isotropy is assumed in the following discussion. Then, the hyperbolic relation is rewritten as

$$Q^{(i)}(\gamma^{(i)}) = [(\gamma^{(i)}/\gamma_v)/(1+|\gamma^{(i)}/\gamma_v|)]Q_v \tag{67}$$

in which Q_v: virtual shear strength and γ_v: virtual reference strain. By substituting into Eq. (44), the virtual tangent stear moduli are obtained for the initial loading as

$$R_L^{(i)} = [1/(1+/|\gamma^{(i)}/\gamma_v|)^2](Q_v/\gamma_v)\Delta\theta \tag{68}$$

It is to be noted in Eqs. (67) and (68) that, though material isotropy is assumed, the superscript (i) for the function Q and R_L is retained because, once unloading become involved, its value will become dependent on the individual history of virtual shear strain.

Details in the rest of the formulation for loading criteria, unloading and reloading will be shown somewhere else (Iai et al, 1990). The formulation is similar to that given for one dimensional analysis by Ishihara et al (1985) for representing the realistic damping factor during the drained cyclic loading. Within the framework of such formulation, the damping factor for each virtual simple shear in the present study is specified by such a function of virtual shear strain amplitude $|\gamma_B^{(i)}|$ as

$$h(|\gamma_B^{(i)}|) = [|\gamma_B^{(i)}/\gamma_h|/(1+|\gamma_B^{(i)}/\gamma_h|)]h_v \tag{69}$$

in which h_v: limiting value of virtual dimping factor when virtual shear strain level is very large; and γ_h: a parameter similar to virtual referense strain.

Four parameters Q_v, γ_v, h_v and γ_h are introduced for modeling shear mechanism. Though these parameters are not directly measurable, they can be readily determined from the well defined soil parameters which are measurable in the laboratory test. First of all, Q_v and γ_v are determined by shear strength τ_m and shear modulus G_m at small strain level. The details in the derivation is shown somewhere else (Iai et al, 1990) but the derivation similar to that by Towhata and Ishihhra (1985 a) yields

$$Q_v = \tau_m/(\sum_{i=1}^{I} \sin\theta_i \Delta\theta) \tag{70}$$

$$\gamma_v = (Q_v/G_m)\sum_{i=1}^{I} \sin^2\theta_i \Delta\theta \tag{71}$$

The soil parameters h_v and γ_h for virtual shear mechanism in Eq. (69) are determined by such a measurable parameter as damping factor of actual simple shear. The details are shown somewhere else (Iai et al, 1990)

7. Scheme for Numerical Robustness

7.1 Problems

When the transient and cyclic loading begins, the excess pore water pressure will build up and the effective mean stress will decrease, changing the values of the shear strength and the shear modulus of soil. If the current values of the shear strength and the shear modulus are determined from the initial values as

$$\tau_m = \tau_{m0}(\sigma_m'/\sigma_{m0}') \tag{72}$$

$$G_m = G_{m0}(\sigma_m'/\sigma_{m0}')^{0.5} \tag{73}$$

they are consistent with the manner in which the initial values depend on the initial effective mean stress in Eqs. (58) and (60). The reference strain for the hyperbolic relation is defined by

$$\gamma_m = \tau_m/G_m \tag{74}$$

so that the reference strain corresponding to the formulation in Eqs. (72) and (73) is given by

$$\gamma_m = \gamma_m(\sigma_m'/\sigma_{m0}')^{0.5} \tag{75}$$

The above formulation, though consistent with the Mohr-Coulomb's failure criterion, poses two problems.

The first problen is the difficulty in the numerical analysis when the effective stress path during cyclic mobility becomes very close to the failure line. Whereas, in the static analysis, a computational artifice such as introduction of virtual visco-plastic term (Zienkiewicz and Cormeau, 1984), is available to overcome this problem, this is not the case in the dynamic analysis. A very small error contained in the computed effective stress causes a very large error in the computed strains, sometimes causing divergence in the solution process. This problem, common to most of the existing models, has been indeed the main obstacle to the two dimensional application of effective stress models in practice.

In practice, meaningful prediction of earthquake induced deformation due to cyclic mobility involve sthe shear strain ranging from about one to ten percent, from which cracks, settlement and other deformation of major consequence initiate. Such a large shear strain, as shown in **Figs. 2** and **3**, is generated only when the effective stress path becomes very close to the failure line. Whereas, in the vicinity of the failure line, the effective stress path apparently converges to a certain limiting stress path, the stress-strain curve does not converge to a closed hysteresis loop; the shear strain rapidly increases in looser sand as shown in **Fig. 2** or gradually and continually increases in denser sand as shown in **Fig. 3**. Some of the existing models, which are successful in simulating the cyclic mobility in the numerically robust manner, do not seem to be very successful in simulating such increase in the shear strain; the stress-strain curve simulated by those models gradually converges to the limiting closed hysteresis loop at the shear strain level ranging from about one to ten percent.

The second problem arising from the formulation by Eqs. (72), (73) and (75) relates to the shape of the hysteresis loop for cyclic loading. The hysteresis loop simulated with this formulation is more of a convex nature even when the stress path is in dilative zone, as shown in **Fig. 8**, than that observed in the laboratory shown in **Fig. 3**. Two effects contribute to the stiffness of soil; as shown in Eq. (68), one being Q_v/γ_v, the other the function of $\gamma^{(i)}/\gamma_v$. Increasing $(-\sigma_m')$ produces increase in G_m and consequently increase in Q_v/γ_v by Eqs. (70) and (71), producing a stiffening in soil. Increasing $\gamma^{(i)}/\gamma_v$, however, produces decrease in the stiffness, resulting in a softening in soil. Thus a mechanism is available for explaining a stiffening with increasing $(-\sigma_m')$ but its effect is too mild, resulting in the unrealistic hysteresis loop.

A scheme is necessary which (1) is numerically robust, (2) simulates the rapid or gradual increase in the shear strain ranging from about one to ten percent although the stress path gradually converges and (3) produces realistic shape in the hysteresis loop.

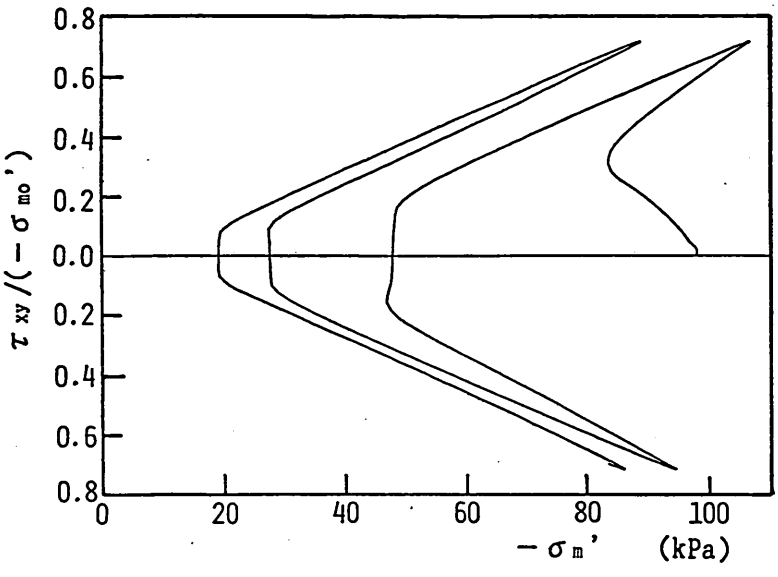

(a) Stress path

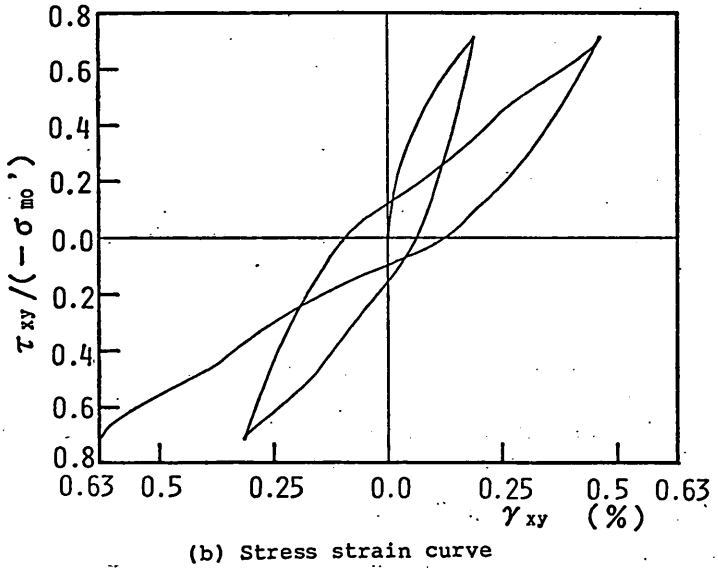

(b) Stress strain curve

Fig 8. Example of problem in shape of hysteresis loop computed by the conventional scheme

7.2 A Simple Scheme

A simple scheme for enhancing the numerical robustness is to introduce additional strength $\Delta\tau_m$ for shear strength. Such a computational artifice is necessary only when the effective stress becomes close to the failure line. As a measure of the "distance" between the failure line and the current effective stress path, the liquefaction front parameter S_0 in Eq. (61) is conveniently used. It is postulated that when $S_0<0.4$ the additional strength is gradually increased with decrease in S_0 as

$$\Delta\tau_m = \Delta r_m(-\sigma_{m0}') \qquad (76)$$

in which

$$\Delta\gamma_m = (m_1 - m_2)(0.4 - S_0) \qquad (77)$$

In the above equation, the term $(0.4-S_0)$ represents the gradual increase and the difference between inclinations of the failure line and the phase transformation line m_1 and m_2 is conveniently chosen as a magnitude of the additional factor.

Introduction of the additional strength produces adverse effect on the shear strain amplitude; the shear strain of the order of few percent will never be achieved or if achieved will result in the closed hysteresis loop. For simulating the rapid or gradual increase in the shear strain ranging from about one to ten percent, another scheme is necessary to overcome such undesirable effect. Let us go back to examine the laboratory data in **Figs. 2** and **3**. If a closer look is directed to these data, it would be possible to recog nize that the rapid or gradual increase in the shear strain amplitude, greater than about one percent, can be approximately simulated by rapidly or gradually enlarging the scale of shear strain axis. Such a scheme as enlarging the scale of shear strain is achieved by recognizing in Eq. (67) that the scale of shear strain is governed by the factor γ_v, which is proportional to the reference strain γ_m. If the reference strain is gradually enlarged, the shear strain will be proportionally enlarged under the same cyclic loading. Because the change in the value of S_0 becomes very small when S_0 approaches zero, the reference strain should be very sensitive to the change in S_0. From this reasoning, it is postulated that when $S_0<0.4$ the reference strain is inversely proportional to $(S_0/0.4)$, such that

$$\gamma_m \propto 1/(S_0/0.4) \qquad (78)$$

For producing realistic shape in the hysteresis loop, it was pointed out earlier that the mechanism for a stiffening with increasing $(-\sigma_m')$ offers only too mild effect; the shear modulus G_m should be more sensitive to the chang in $(-\sigma_m')$. From this reasoning, it is postulated that the current value of the shear modulus during cyclic mobility is proportional to (σ_m'/σ_{m0}'), such that

$$G_m \propto (\sigma_m'/\sigma_{m0}') \qquad (79)$$

From the conditions given by Eqs. (76) through (79), the formulation analogous to Eqs. (72), (73) and (75) will be obtained as a simple scheme for robust simulation of cyclic mobility. To begin, when with $S_0>0.4$, no correction is applied for shear strength so that the shear strength is given by Eq. (72), such that

$$\tau_m = \tau_{m0}(\sigma_m'/\sigma_{m0}') \qquad (\text{if } S_0>0.4) \qquad (80)$$

From the condition in Eq. (79), the shear modulus during cyclic mobility is given by

$$G_m = G_{m0}(\sigma_m'/\sigma_{m0}') \qquad (\text{if } S_0>0.4) \qquad (81)$$

Thus, the reference strain is given by

$$\gamma_m = \gamma_{m0} \qquad (\text{if } S_0>0.4) \qquad (82)$$

When $S_0<0.4$, the factor $\Delta\tau_m$ defined in Eqs. (76) and (77) should be added to the shear strength, such that

$$\tau_m = \tau_{m0}(\sigma_m'/\sigma_{m0}') + \Delta\tau_m \qquad (\text{if } S_0<0.4) \qquad (83)$$

From the condition in Eq. (78) and the relation in Eq. (82), the reference strain is given by

$$\gamma_m=\gamma_{m0}/(S_0/0.4) \qquad (\text{if } S_0<0.4) \tag{84}$$

Therefore, the shear modulus during cyclic mobility is given as

$$G_m=\tau_m/\gamma_m \qquad (\text{if } S_0<0.4) \tag{85}$$

In theory when the liquefaction parameter S_0 reaches the limiting value S_1 in Eq. (61), the hysteresis loop becomes closed loop. Such limit, in practice, can be chosen so as to produce a shear strain amplitude of more than a hundred percent as the limlting case; then the existence of limit does not cause a problem in practice. It is further to be noted that in the present scheme S_0 serving as a scaling factor for the shear strain amplitude is determined by a function of accumulated plastic shear work so that the computed shear strain is insensitive against sporadically arising, if any, errors during the computation process.

The present scheme is further simplified under undrained condition. Under undrained condition, the state variable S in Eq. (52) is approximately equal to (σ_m'/σ_{m0}'). If it is realized that, after all, the relations in Eqs. (80) through (85) are a computational artifice which approximates the relation in reality, it can be justified to use further approximation that S is used on behalf of (σ_m'/σ_{m0}') in Eqs. (80) through (85). The use of the state variable S further enhances the efficiency and the stability of the numerical solution because S is directly determined from the accumulated plastic shear work and the shear stress ratio. Such an efficient scheme is given by

When $S_0>0.4$

$$\tau_m=\tau_{m0}S \tag{86}$$

$$G_m=\tau_m/\gamma_{m0} \tag{87}$$

$$\gamma_m=\gamma_{m0} \tag{88}$$

When $S_0<0.4$

$$\tau_m=\tau_{m0}S+\Delta\tau_m \tag{89}$$

$$G_m=\tau_m/\gamma_m \tag{90}$$

$$\gamma_m=\gamma_{m0}/(S_0/0.4) \tag{91}$$

in which $\Delta\tau_m$ is defined in Eq. (76) and (77). It is to be noted that the sheme for enlarging the scale of shear strain is applicable only for the process in which S_0 monotonically decreases such as undrained or partially drained condition. For the process in which S_0 involves increasing as well as decreasing processes, it would be necessary to introduce an additional scheme for appropriately memorizing the previous history of S_0 and its effects. To develop such a scheme is beyond the scope of the present study.

8. Model Performance

The model presented in this pape is coded into the finite element computer program FLIP (Finite element analysis of Liquefaction Program) and is used for examining the overall performance of the present approach. The basic steps in the computation are (1) to compute the displacement increment from the nodal force increment by using the incremental relation in Eq. (30) or (32) and (2) to compute the nodal force from the computed displacement by using the integrated relation in Eq. (48). Convergence to the stress strain relation in Eq. (48) is ensured by the use of correction force as well as iteration. The scheme in Eqs. (86) through (91) is used for assuring the numerical robustness. All the results to be presented here are computed as a solution of a stress controlled boundary value problem by using one element. Thus, the numerical robustness of the model is more critically examined here than in case of strain controlled computation.

The undrained torsion shear tests with initially isotropically consolidated sand shown in **Figs. 2** and **3** are simulated with the parameters shown in **Table 1**. The parameters are obtained by the back-fitting. The computed results are shown in **Figs. 9** an **10**, indicating good agreements with the laboratory test results for both looser and denser sand.

Table 1 Perameters for the model

Parameters	Loose Fuji River sand (D_r=47%)	Dense Fuji River Sand (D_r=75%)
K_{ma}	270, 500 kPa	366, 800 kPa
G_{ma}	103, 700 kPa	140, 700 kPa
p_1	0. 45	0. 45
p_2	1. 4	0. 72
w_1	2. 0	2. 85
S_1	0. 0035	0. 005
c_1	1. 0	1. 0
$\sin\phi_f'$	0. 87	0. 91
$\sin\phi_p'$	0. 42	0. 42
h_v	0. 3	0. 3
n	0. 45	0. 40
K_f	2.0×10^6 kPa	2.0×16^6 kPa

K_{ma} and G_{ma} are given for $(-\sigma_{ma}')=98$ kPa. The computation was done with number of the shear mechanism I=12 by 50 steps of incremental loading for 1/4 cycle.

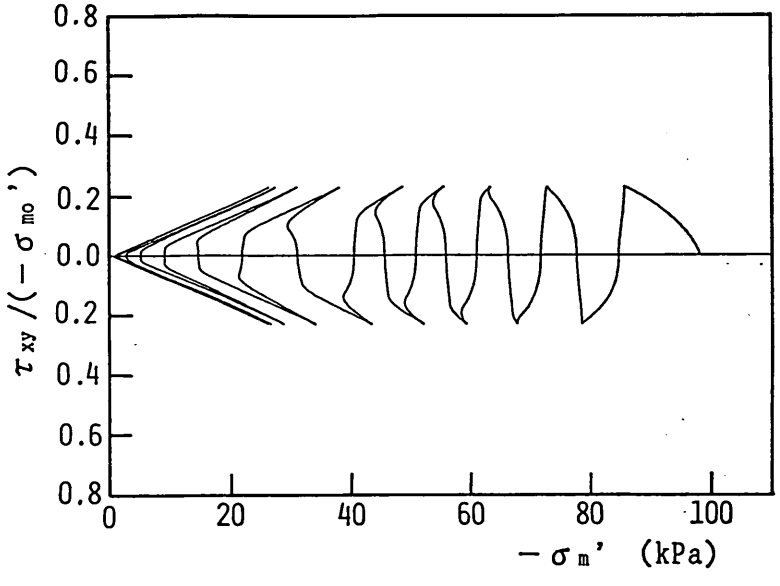

(a) Stress path

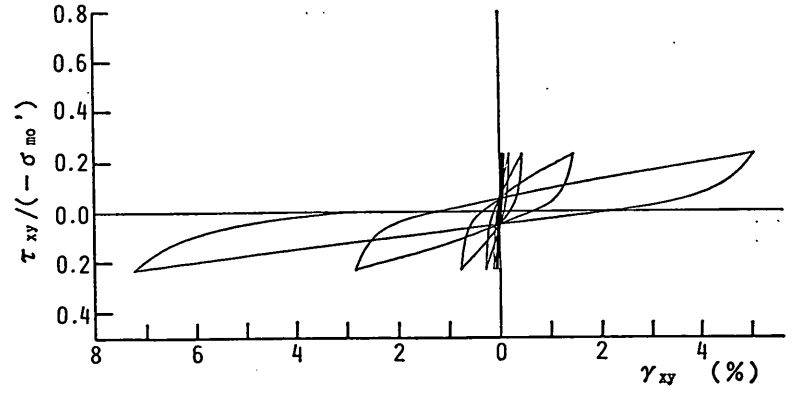

(b) Stress strain curve

Fig. 9 Computed results of loose sand to be compared with the laboratory results in Fig. 2.

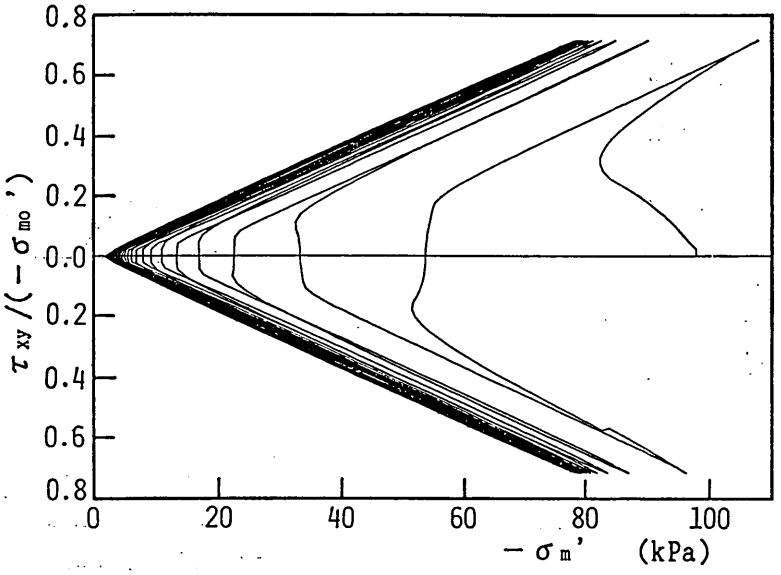

(a) Stress path

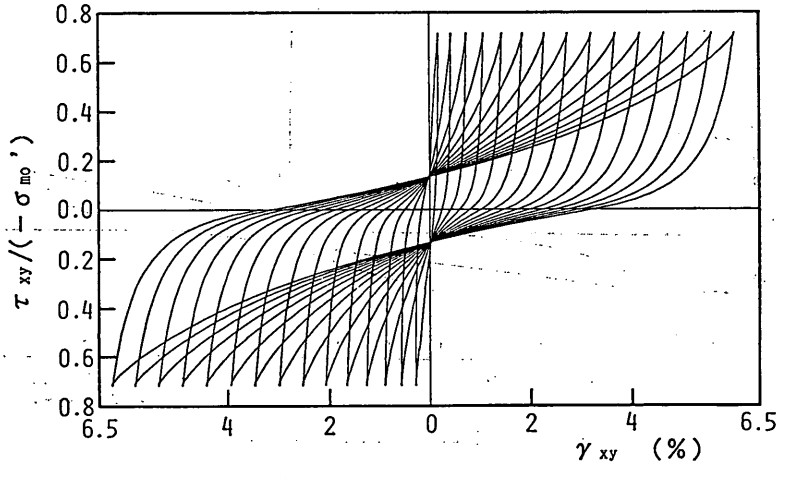

(b) Stress strain curve

Fig. 10 Computed results of dense sand to be compared with the laboratory results in Fig. 3.

9. Conclusions

An attempt made for modeling cyclic mobility of saturated cohesionless soil. The proposed concept is of a generalized plasticity type defined in strain space. The concept of multiple mechanism is used as a vehicle for decomposing the complex mechanism into a set of simple mechanisms defined in one dimensional space. Incremental as well integrated constitutive relations are obtained. In particular, the tangent stiffness matrix in the incremental relation becomes symmetric, ensuring the efficiency in the numerical analysis, whereas the integrated constitutive relation serves as a guide, ensuring the convergence to the realistic stress strain relation. Number of the parameters for the proposed model is ten if two obvious parameters, i.e. porosity of soil skeleton and bulk modulus of pore water, are omitted in counting number of the parameters.

Difficulty is known to exist in the numerical analysis of cyclic mobility when the effective stress path becomes very close to the failue line. In order to overcome such difficulty, a simple scheme is proposed; modeling of cyclic mobility, not as a yielding process, but as a process in which the scale of the shear strain is gradually enlarged with progress of cyclic mobility. The rapid as well as well as persistent increase in the shear strain amplitude greater than several percent is simulated in the numerically robust manner.

Acknowledgments

The authors wish to thank Profs. K. Ishihara and I. Towhata at Tokyo University for their valuable discussions.

References

1) Castro, G. (1975): "Liquefaction and cyclic mobility of saturated sand," *Journal of Geotechnical Engineering Divison*, ASCE, Vol. 101, No. GT6, pp. 551-569
2) Dobry, R., Ladd, R. S., Yokel, F. Y., Chung, R. M. and Powell, D. (1982): "Prediction of pore water pressure buildup and liquefaction of sands during earthquakes by the cyclic strain method," *NBS Building Science Series 138*, National Bureau of Standards, U. S. Department of Commerce, 150p.
3) Iai, S., Matsunaga, Y. and Kameoka, T. (1990); "Parameter identification for a cyclic mobility model," *Report of Port and Harbour Research Institute*, Vol. 29, No. 4
4) Isihara, K. (1985): "Stability of natural deposits during earthquaks," *Proceedings of 11th International Conference on Soil Mechanics and Foundation Engineering*, San Francisco, Vol. 1, pp. 327-376
5) Ishihara, K., Tatsuoka, F. and Yasuda, S. (1975): "Undrained deformation of sand under cyclic stresses," *Soils and Foundations*, Vol. 15, No. 1, pp. 29-44
6) Ishihara, K. and Towhata, I. (1982): "Dynamic response analysis of level ground based on the effective stress method," in Pande, G. N. and Zienkiewicz, O. C. eds., *Soil Mechanics-Transient and Cyclic Loads*, John Wiley and Sons, pp. 133-172
7) Ishihara, K., Yoshida, N. and Tsujino, S. (1985): "Modelling of stress-strain relations of soils in cyclic loading," *Proceedings of 5th Conference on Numerical Methods in Geomechanics*, Nagoya, Vol. 1, pp. 373-380

8) Mroz, Z. and Norris, V. A. (1982) : "Elastoplastic and viscoplastic constitutive models for soils," in Pande, G. N. and Zienkiewicz, O. C. (eds), *Soil Mechanics-Transient and Cyclic Loads*, Chapter 8, John Wiley and Sons, pp. 173-217
9) Pender, M. J. (1980) : "Cyclic mobility— a critical state model," *Proceedings of International Symposium on Soils under Cyclic and Transient Loading*, Swansea, Vol. 1, pp. 325-333
10) Towhata, I. and Ishihara, K. (1985 a) : "Modelling soil behaviour under principal stress axes rotation," *Proceedings of 5th International Conference on Numerical Methods in Geomechanics*, Nagoya, Vol. 1, pp. 523-530
11) Towhata, I. and Ishihara, K. (1985 b) : "Shear work and pore water pressure in undrained shear," *Soils and Foundations*, Vol. 25, No. 3, pp. 73-84
12) Yamazaki, F., Towhata, I. and Ishihara, K. (1985) : "Numerical model for liquefaction problem under multidirectional shearing on horizontal plane," *Proceedings of 5th International Conference on Numerical Methods in Geomechanics*, Nagoya, Vol. 1, pp. 399-406
13) Zienkiewicz, O. C., Chang, C. T. and Hinton, E. (1978) : "Nonlinear seisimic response and liquefaction," *International Journal for Numerical and Analytical Methods in Geomechanics*, Vol. 2, pp. 381-404
14) Zienkiewicz, O. C. and Cormeau, I. C. (1984) : "Viscoplasticity —plasticity and creep in elastic solids— a unified numerical solution approach," *International Journal for Numerical Methods in Engineering*, Vol. 8, pp. 821-845

Appendix

The correction factor R to be multiplied with dW_S is basically given by

$$R=(m_1-r/S)/(m_1-m_3) \qquad (\text{if } r/S>m_3) \tag{A1}$$

When S becomes small, however, the value of r/S becomes so sensitive to the small errors contained in the values of r and S that R given by Eq. (A1) becomes numerically unreliable. Therefore, a measure is taken for small values of S, such that, if $S<0.4$, R is given by

$$R=(m_1-r/0.4)/(m_1-m_3) \qquad (\text{if } r/S>m_3) \tag{A2}$$

The most of the effect of the above correction might be, however, offset by the parameter p_2 in Eq. (59).

Notation

$B=[K_a/(-\sigma_{ma}')^{0.5}]^2$: factor for volumetric relation
c_1 : parameter for specifying the level of threshold limit
$\boldsymbol{D}$: tangential stiffness matrix
$\boldsymbol{D}_{L/U}{}^{(i)}$: tangential stiffness matrix for mechanism i at loading and unloading
$\boldsymbol{e}^T=[(\varepsilon_x+\varepsilon_y), (\varepsilon_x-\varepsilon_y), \gamma_{xy}]$: transformed strain
$\boldsymbol{e}_p{}^T=(\varepsilon_p, 0, 0)$: additional volumetric strain of plastic nature in transformed space
G_{m0} : initial shear modulus
$G_m{}^*$: shear modulus used for computing plastic shear work
G_m : shear modulus

h : damping factor for virtual simple shear
h_v : limiting virtual damping factor
I : number of the multiple mechanism for shear
K : elastic tangent bulk modulus of soil skeleton
K_a : value of K at $\sigma_m' = \sigma_{ma}'$
K_f : bulk modulus of pore water
$\boldsymbol{l}^{(i)}$ and $\boldsymbol{l}_{L/U}{}^{(i)}$: transformed vectors of $\boldsymbol{n}^{(i)}$ and $\boldsymbol{n}_{L/U}{}^{(i)}$
$m_1 = \sin\phi_f'$: inclination of failure line
$m_2 = \sin\phi_p'$: inclination of phase transformation line
$m_3 = 0.67 m_2$: auxiliary parameter
$\boldsymbol{n}^{(i)}$: loading/unloading direction vector for mechanism i
$\boldsymbol{n}_{L/U}{}^{(i)}$: direction vectors of stress increments for mechanism i at loading and unloading
n : porosity of soil skeleton
p_1, p_2, w_1, S_1 : material parameters for dilatancy
$Q^{(i)}$: virtual shear stress per unit angle for mechanism i
$Q^{(i)}{}_B$: virtual simple shear stress amplitude per unit angle
Q_v : virtual shear strength per unit angle
r : state variable equivalent to τ/σ_{m0}'
R : correction factor for cumulative shear work in dilative zone
$R_{L/U}{}^{(i)}$: tangential stiffness modulus for mechanism i at loading and unloading
S : state variable equivalent to σ_m'/σ_{m0}'
S_0 : liquefaction front parameter
$\boldsymbol{s}'^T = [(\sigma_x'+\sigma_y')/2,\ (\sigma_x'-\sigma_y')/2,\ \tau_{xy}]$: transformed stress
$\boldsymbol{T}_\varepsilon$: transformation matrix for strain
$\boldsymbol{T}_\sigma$: transformation matrix for stress
u, v : displacements in x and y directions
W_n : factor for normalization of shear work
W_s : plastic shear work
W_{st} : total shear work
W_{se} : elastic shear work
$W^{(i)}$: equivalent elastic virtual strain energy for mechanism i
w : normalized shear work
$\gamma^{(i)}$: virtual simple shear strain for mechanism i
γ_{m0} : initial reference strain
γ_m : reference strain
γ_h : a parameter for damping factor similar to virtual reference strain
γ_v : virtual reference strain
γ_{xyB} : amplitude of simple shear strain
$\gamma^{(i)}{}_B$: amplitude of virtual simple shear strain for mechanism i
$\boldsymbol{\varepsilon}^T = (\varepsilon_x,\ \varepsilon_y,\ \varepsilon_{xy})$: strain
ε_p : additional volumetric strain of plastic nature
ε_e : elastic volumetric strain
ε_{e0} : initial elastic volumetric strain
$\theta_i = (i-1)\Delta\theta$: angle for virtual shear mechanism i in $(\varepsilon_x-\varepsilon_y)-\gamma_{xy}$ plane
$\Delta\theta = \pi/I$
$\boldsymbol{\sigma}'^T = (\sigma_x',\ \sigma_y',\ \sigma_{xy})$: effective stress
$\boldsymbol{\sigma}'^{(i)}$: virtual stress for machanism i
$\sigma_m' = (\sigma_x'+\sigma_y')/2$: mean effective stress
σ_{m0}' : initial mean effective stress
$\tau = (\sigma_1'-\sigma_3')/2$: deviatoric stress
τ_m : shear strength

τ_{m0} : initial shear strength
ϕ_f' : shear resistance angle
ϕ_p' : phase transformation angle